Proceedings of DETC'01
ASME 2001 Design Engineering Technical Conferences
and Computers and Information in Engineering Conference
Pittsburgh, Pennsylvania, September 9-12, 2001

DETC2001/DAC-21030

STRUCTURAL OPTIMIZATION OF A SPHERICAL PARALLEL MANIPULATOR USING A TWO-LEVEL APPROACH

Florence Bidault,
Departement of Industrial and
Mechanical Engineering
Ecole Centrale de Nantes
France
Email: Florence.Bidault@irccyn.ec-nantes.fr

Chin-Pun Teng and Jorge Angeles
Department of Mechanical Engineering &
Centre for Intelligent Machines
McGill University
Montreal, Quebec, H3A 2K6
Canada
Email:chinpunt@cim.mcgill.ca, angeles@cim.mcgill.ca

ABSTRACT

The Agile Wrist, a spherical wrist with a parallel, isotropic architecture for highest orientational accuracy, is being designed as a module of an 11-degree-of-freedom (dof) robot.

The wrist consists of two main elements, the base and the moving plates. The two plates are coupled by means of three identical legs, each of these composed of two links, proximal and distal, coupled to each other by a revolute joint. Each leg, in turn, is coupled to its proximal plate via revolute joints. Moreover, the three axes of the leg-revolute joints are concurrent at the center of the wrist, each axis making an angle of 90° with its neighbor. Direct-drive DC motors are used to rotate the wrist proximal links and electrical brakes and optical encoders are located on each of the motor shafts for control purposes.

In this paper we introduce a two-level approach to the optimum design of the proximal link of the Agile Wrist. First, the shape of the midcurve producing minimum stress concentrations is obtained by means of the concept of *curve synthesis* using cubic splines. At the second level, the optimum cross-section along the midcurve producing a link of minimum weight is determined.

Figure 1. A RENDERING OF THE AGILE WRIST

INTRODUCTION

The Agile Wrist (AW), shown in Figure 1, is the three-dof orienting module of the redundant, 11-axis Multi-Modular Manipulator (M^3) currently under design at McGill University's Centre for Intelligent Machines (Angeles et al, 1999). It owes its name to the *Agile Eye* (AE) developed by Gosselin and his team at Université Laval, Quebec, Canada (Gosselin and Lavoie, 1993; Gosselin and Hamel, 1994; Gosselin and Gagné, 1995). However, while keeping the advantages of a parallel, isotropic architecture for highest orientation accuracy, the AW has a lighter

weight as compared to the AE; moreover, the AW avoids collisions between the tool installed on top of the mobile platform and the moving links. A robot architecture is said to be isotropic if it allows for robot postures whereby the Jacobian matrix has all its singular values identical and nonzero.

The AW consists of two plates coupled by three identical legs. Each leg is composed of two links, the proximal and the distal, coupled to each other by means of a revolute joint. The shapes of the midcurves of the distal links are restricted to be circular arcs, whereas those of the proximal links are only shape-constrained at their two ends. Since the design of the distal link is rather simple, we focus in this paper on the optimum design of the midcurve and the cross-section of the proximal link.

In the design of the proximal link, we aim at minimizing the weight while avoiding stress concentrations. The design consists of two levels: (i) finding the shape of the midcurve which renders minimum the stress concentrations and (ii) determining the cross-section which minimizes the overall weight subject to a maximum allowable stress. The midcurve is obtained by means of the concept of *curve synthesis* (Angeles, 1983) using cubic splines; the optimization problem thus resulting is then solved with the aid of the ODA package (Teng, and Angeles, 2000). Next, we resort to finite element analysis (FEA) and structural optimization, by means of *ProMechanica* to solve the problem of determining the cross-section along the midcurve that produces a link of minimum weight subject to the maximum allowable stress.

KINETOSTATIC ANALYSIS

While the kinematic analysis of parallel spherical wrists has been the subject of many publications, the static analysis has received less attention. Yi, Freeman and Tesar (1992) proposed a force and stiffness transmission analysis for a spherical shoulder mechanism by means of the Jacobian matrix. This kind of analysis provides the designer with useful information to select the appropriate actuators, but in the case of spherical wrists, only moments are taken into account by the analysis, the forces at the joints remaining indeterminate. While designing the links of the *Agile Wrist*, we had to be sure that they can withstand the load of the tool, but no moments are created if this load is directed along a line passing through the center of the wrist, which is the case when the *Agile Wrist* is in its nominal posture, with its base oriented horizontally.

In our case, the base of the *Agile Wrist* can be oriented vertically; in this orientation, it is then possible to determine the moment exerted by the weight of the tool at the centre of the wrist by using a Jacobian approach and then evaluating the loading moment that acts on the most heavily loaded leg. The ensuing kinetostatic analysis enables us to determine which maximum moment magnitude the *Agile Wrist* can withstand using the prescribed actuators.

Kinematics of the Agile Wrist and of the i^{th} Leg

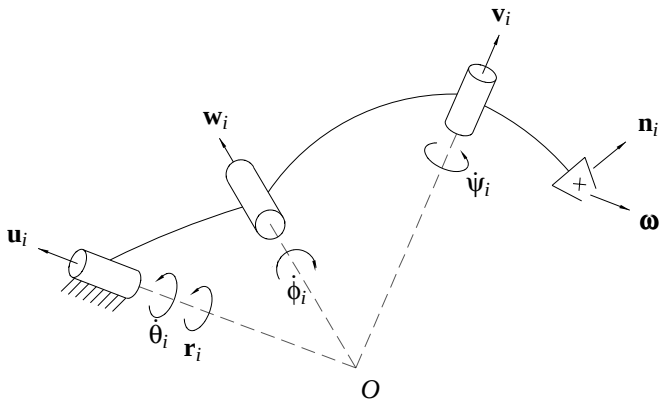

Figure 2. THE i_{th} LEG OF THE AW

Each leg of the *Agile Wrist* is a serial RRR spherical wrist, as shown in Fig. 2. This serial wrist is orthogonal, i.e., its neighboring revolute axes are laid out at 90°. The angular velocity $\boldsymbol{\omega}$ of the end effector of the *Agile Wrist* can be expressed as a function of the joint rates of the i^{th} leg, i.e.,

$$\dot{\theta}_i \mathbf{u}_i + \dot{\phi}_i \mathbf{w}_i + \dot{\psi}_i \mathbf{v}_i = \boldsymbol{\omega} \tag{1}$$

To eliminate the unactuated rates of the previous expression, eq.(1) is dot-multiplied by the cross-product $\mathbf{w}_i \times \mathbf{v}_i$, namely,

$$\dot{\theta}_i (\mathbf{w}_i \times \mathbf{v}_i) \cdot \mathbf{u}_i = (\mathbf{w}_i \times \mathbf{v}_i) \cdot \boldsymbol{\omega} \tag{2}$$

Upon assembling the scalar equations (2) for $i = 1, 2, 3$, we have

$$\mathbf{B}\dot{\boldsymbol{\theta}} = \mathbf{A}\boldsymbol{\omega} \tag{3}$$

where $\boldsymbol{\theta} = [\dot{\theta}_1 \ \dot{\theta}_2 \ \dot{\theta}_3]^T$ is the vector of actuated joint rates at the base of the AW, and matrices $\mathbf{A}$ and $\mathbf{B}$ are defined as

$$\mathbf{A} = \begin{bmatrix} (\mathbf{v}_1 \times \mathbf{w}_1)^T \\ (\mathbf{v}_2 \times \mathbf{w}_2)^T \\ (\mathbf{v}_3 \times \mathbf{w}_3)^T \end{bmatrix} \tag{4a}$$

and

$$\mathbf{B} = \mathrm{diag}[\mathbf{u}_1 \times \mathbf{w}_1 . \mathbf{v}_1, \ \mathbf{u}_2 \times \mathbf{w}_2 . \mathbf{v}_2, \ \mathbf{u}_3 \times \mathbf{w}_3 . \mathbf{v}_3] \tag{4b}$$

If $\mathbf{B}$ is nonsingular, then

$$\dot{\boldsymbol{\theta}} = -\mathbf{B}^{-1}\mathbf{A}\boldsymbol{\omega} \tag{5}$$

Assuming $\mathbf{n}$ to be the moment acting on the end-effector, taken at the center of the wrist, and $\boldsymbol{\tau}$ the vector array of actuator torques, the power developed by the load and the motors, Π_e and Π_m is, respectively,

$$\Pi_e = \mathbf{n}^T\boldsymbol{\omega}, \qquad \Pi_m = \boldsymbol{\tau}^T\dot{\boldsymbol{\theta}} \tag{6}$$

From the Principle of Virtual Work, under kinetostatic, conservative conditions, we obtain

$$\mathbf{n}^T\boldsymbol{\omega} = \boldsymbol{\tau}^T\dot{\boldsymbol{\theta}} \tag{7}$$

Upon substituting eq.(5) into eq.(7), we thus have, for any $\boldsymbol{\omega}$,

$$\mathbf{n} = -\mathbf{A}^T\mathbf{B}^{-T}\boldsymbol{\tau} \quad \Rightarrow \quad \boldsymbol{\tau} = -\mathbf{B}\mathbf{A}^{-1}\mathbf{n} \tag{8}$$

Moreover, $\mathbf{n}$ is distributed among all three legs, with the i^{th} leg taking up a part $\mathbf{n}_i$ of $\mathbf{n}$, i.e.,

$$\mathbf{n} = \mathbf{n}_1 + \mathbf{n}_2 + \mathbf{n}_3 \tag{9}$$

Let $\boldsymbol{\mu}_i = [\tau_i\ 0\ 0]^T$ be the three-dimensional joint-torque vector of the i^{th} leg. We have

$$\mathbf{J}_i{}^T\mathbf{n}_i = \boldsymbol{\mu}_i \tag{10}$$

where $\mathbf{J}_i$ is the ith-leg Jacobian matrix, defined as

$$\mathbf{J}_i = [\mathbf{u}_i\ \mathbf{w}_i\ \mathbf{v}_i] \tag{11}$$

Upon inverting eq.(10), we obtain

$$\mathbf{n}_i = \mathbf{J}_i{}^{-T}\boldsymbol{\mu}_i \tag{12}$$

which is the share of the load taken up by the i^{th} leg. To calculate $\mathbf{J}_i{}^{-1}$, reciprocal bases (Brand 1965) can be used, thus obtaining

$$\Delta_i = \det(\mathbf{J}_i) = \mathbf{u}_i \times \mathbf{w}_i \cdot \mathbf{v}_i \tag{13a}$$

and

$$\mathbf{J}_i{}^{-1} = \frac{1}{\Delta_i}\begin{bmatrix} (\mathbf{w}_i \times \mathbf{v}_i)^T \\ (\mathbf{v}_i \times \mathbf{u}_i)^T \\ (\mathbf{u}_i \times \mathbf{w}_i)^T \end{bmatrix} \tag{13b}$$

whence,

$$\mathbf{n}_i = \mathbf{J}_i{}^{-1}\boldsymbol{\mu}_i = \frac{\tau_i}{\mathbf{u}_i \times \mathbf{w}_i.\mathbf{v}_i}\mathbf{w}_i \times \mathbf{v}_i \tag{14}$$

The load $\mathbf{n}_i$ taken by one leg is thus normal to the plane defined by the second and third-revolute axes of the i^{th} leg. This could not be otherwise, for each of these revolutes being unactuated, it can exert a moment on the links that it connects only in a direction lying in a plane normal to its axis. Moreover, the moment exerted by the end-effector onto the distal link must be equal and of opposite sign to that exerted by the proximal link onto the same distal link, under the equilibrium of forces.

Load Moment Acting on the Most Heavily Loaded Leg

We consider a loading condition in which the base of the AW is oriented vertically and the AW is in its nominal isotropic posture, as depicted in Fig. 3; the most heavily loaded leg appears here to be the second leg.

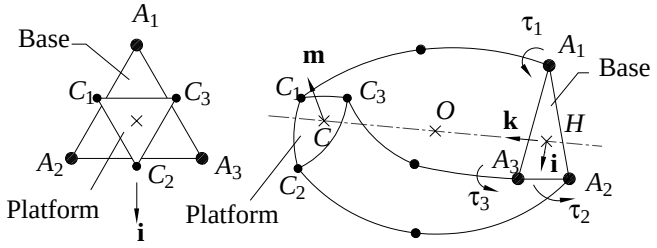

Figure 3. POSTURE OF THE AW FOR THE KINETOSTATIC ANALYSIS

As depicted in Fig. 3, we assumed that the weight of the tool and the moving platform is concentrated at the center of the moving platform, C, with O denoting the center of the wrist and C_i the center of the revolute joint coupling the i^{th} leg with the moving platform. The distance between O and C_i is denoted by R_m. The force vector at point C is noted $\mathbf{f} = F\mathbf{i}$ and the vector pointing from O to C is noted $\mathbf{c} = R_m\mathbf{k}$; vector $\mathbf{i}$, directed along the vertical, is in a plane parallel to the base, and vector $\mathbf{k}$, directed along the horizontal, is collinear with a line passing through H, the center of the base, and O. The unit vectors $\mathbf{u}_i$, $i = 1,2,3$, form an orthonormal frame U which will be used henceforth. The nominal

configuration for the distal vectors is characterized by

$$\mathbf{v}_{10} = -\mathbf{u}_3, \qquad \mathbf{v}_{20} = -\mathbf{u}_1, \qquad \mathbf{v}_{30} = -\mathbf{u}_2 \tag{15}$$

and for the intermediate unit vectors by

$$\mathbf{w}_{10} = \mathbf{u}_2, \qquad \mathbf{w}_{20} = \mathbf{u}_3, \qquad \mathbf{w}_{30} = \mathbf{u}_1 \tag{16}$$

In the frame $U(O, \mathbf{u}_1, \mathbf{u}_2, \mathbf{u}_3)$, the coordinates of the points A_1 and H are $(d\ ,\ 0\ ,\ 0)$ and $(d/3\ ,\ d/3\ ,\ d/3)$, respectively. Since vector $\mathbf{k}$ has the same direction as the vector pointing from H to O, and vector $\mathbf{i}$ the same one as the vector pointing from A_1 to H, vectors $\mathbf{k}$ and $\mathbf{i}$ are readily obtained after a normalization process. Vector $\mathbf{j}$ can then be obtained by means of the cross product: $\mathbf{j} = \mathbf{k} \times \mathbf{i}$.

$$\mathbf{k} = -\frac{\sqrt{3}}{3}\mathbf{u}_1 - \frac{\sqrt{3}}{3}\mathbf{u}_2 - \frac{\sqrt{3}}{3}\mathbf{u}_3 \tag{17}$$

$$\mathbf{i} = -\frac{\sqrt{6}}{3}\mathbf{u}_1 + \frac{\sqrt{6}}{6}\mathbf{u}_2 + \frac{\sqrt{6}}{6}\mathbf{u}_3 \tag{18}$$

The moment $\mathbf{n}_O$ with respect to the center of the wrist is given by

$$\mathbf{n}_O = \mathbf{c} \times \mathbf{f} + \mathbf{n}_C \tag{19}$$

where $\mathbf{n}_C$ is the load moment vector with respect to point C, here considered equal to zero. From eq.(19) we obtain

$$\mathbf{n}_O = R_m F(\mathbf{i} \times \mathbf{k}) \tag{20}$$

We determine the torque at each actuated joint with relation (8). For the nominal configuration, $-\mathbf{B}\mathbf{A}^{-1}$ corresponds to the 3×3 identity matrix. Equations (8) and (14) lead to:

$$\boldsymbol{\tau}_0 = \mathbf{n}_0 \tag{21}$$

and

$$\mathbf{n}_{i_0} = \tau_{i0}\mathbf{u}_i \tag{22}$$

where τ_{i0} given by

$$\tau_{i0} = R_m F(\mathbf{i} \times \mathbf{k}) \cdot \mathbf{u}_i = \frac{\sqrt{2}}{2} R_m F \tag{23}$$

The moment at the distal joint coupling the distal link with the moving platform is, then,

$$\mathbf{n}_{i_0} = \frac{\sqrt{2}}{2} R_m F \mathbf{u}_i \tag{24}$$

According to Servo Systems, of Montville, NJ, the manufacturer of the *Agile Wrist* direct-drive motors, these can provide a peak torque of 0.353 Nm. Relation (8) enables us to determine the moments that the *Agile Wrist* can balance for eight different cases:

$$\tau_1 = \pm 0.353 \text{ Nm}, \ \tau_2 = \pm 0.353 \text{ Nm and } \tau_3 = \pm 0.353 \text{ Nm}$$

For the nominal configuration, eq.(8) yields the moment:

$$\mathbf{n}_O = \tau_1\mathbf{u}_1 + \tau_2\mathbf{u}_2 + \tau_3\mathbf{u}_3 \tag{25}$$

The components of the moment $\mathbf{n}_O$ in frame $V(O, \mathbf{i}, \mathbf{j}, \mathbf{k})$ are

$$M_x = \tau_1\frac{\sqrt{3}}{3} - \tau_2\frac{\sqrt{3}}{3} - \tau_3\frac{\sqrt{3}}{3} \tag{26}$$

$$M_y = \tau_2\frac{\sqrt{2}}{2} - \tau_3\frac{\sqrt{2}}{2} \tag{27}$$

$$M_z = -\tau_1\frac{\sqrt{6}}{3} + \tau_2\frac{\sqrt{6}}{6} + \tau_3\frac{\sqrt{6}}{6} \tag{28}$$

If we suppose that the moment about the center of the wrist is only due to the weight of the tool that acts at the centroid of the moving platform that is, $|M_y| = R_m F$, then the mass of the tool that this manipulator can support is about 0.7 kg (R_m is about 74 mm, the radius of the distal link). However, this estimate is done for the worst loading condition, i.e., with the base oriented vertically.

STATIC ANALYSIS

The *Agile Wrist* is composed of seven moving links: the moving platform, three distal links and three proximal links. These links are coupled by revolute joints. We thus have nine revolute joints in the whole mechanism and $9 \times 5 = 45$ unknown reaction components. Indeed, by virtue of the nature of revolute joints, the moment about any point along each unactuated joint axis is zero. By the same token, the moment about an actuated revolute is known. Upon applying the static equilibrium conditions, we obtain $7 \times 6 = 42$ equations, the problem thus being statically indeterminate. To solve it, we need additional information or engineering hypotheses. In fact, we decided to solve the indeterminacy by replacing, both in the mold and in the design, the unactuated revolute joints by cylindrical joints. The moment component about any point along each cylindrical joint is equal to that of the corresponding revolute but now also the force along the axis of

the cylindrical joint is zero. The number of unknowns is then reduced to $3\times5+6\times4=42$ and the system becomes determinate. Such an approach was also adopted by Larochelle and McCarthy (1992) while discussing the static analysis of spherical *nR* kinematic chains with joint friction. Even if they did not aim at replacing the revolute joints by cylindrical joints, they stated that due to the geometry of the joints, no force is transmitted along the axis of unactuated joints. It is to be noticed that such changes do not have any effect on the kinematics of the *Agile Wrist*; moreover, they avoid overconstraints and ease the assembly of the mechanism.

Static Analysis of the Proximal Links

For the purpose of optimization, we conduct a static analysis, whereby all links are assumed rigid and two types of forces are considered: those exerted by the environment, e.g. the weight of the moving platform and the tool, and those coming from the kinematic joints. The weight of the proximal links is neglected. Let $\mathbf{f}_{dp_i}=[X_{dp_i}\ \ Y_{dp_i}\ \ Z_{dp_i}]^T$ and $\mathbf{f}_{bp_i}=[X_{bp_i}\ \ Y_{bp_i}\ \ Z_{bp_i}]^T$ be the forces exerted by the i^{th} distal link on the i^{th} proximal link at point K_i, and by the base on the i^{th} proximal link at point B_i, respectively. Moreover, $\mathbf{m}_{md_i}=[U_{md_i}\ \ V_{md_i}\ \ W_{md_i}]^T$ and $\mathbf{m}_{bp_i}=[U_{bp_i}\ \ V_{bp_i}\ \ W_{bp_i}]^T$ denote the moment about C_i exerted by the moving platform on the i^{th} distal link and the moment about B_i exerted by the base on the i^{th} proximal link, respectively. The wrenches exerted by the distal link on the proximal link $\mathbf{w}_{dp_i}$ and those exerted by the base on the proximal link, $\mathbf{w}_{bp_i}$, are thus,

$$\mathbf{w}_{dp_1}=\begin{bmatrix}U_{dp_1}\\0\\W_{dp_1}\\X_{dp_1}\\0\\Z_{dp_1}\end{bmatrix}\quad \mathbf{w}_{dp_2}=\begin{bmatrix}U_{dp_2}\\V_{dp_2}\\0\\X_{dp_2}\\Y_{dp_2}\\0\end{bmatrix}\quad \mathbf{w}_{dp_3}=\begin{bmatrix}0\\V_{dp_3}\\W_{dp_3}\\0\\Y_{dp_3}\\Z_{dp_3}\end{bmatrix}$$

$$\mathbf{w}_{bp_1}=\begin{bmatrix}0\\V_{bp_1}\\W_{bp_1}\\X_{bp_1}\\Y_{bp_1}\\Z_{bp_1}\end{bmatrix}\quad \mathbf{w}_{bp_2}=\begin{bmatrix}0\\V_{bp_2}\\W_{bp_2}\\X_{bp_2}\\Y_{bp_2}\\Z_{bp_2}\end{bmatrix}\quad \mathbf{w}_{bp_3}=\begin{bmatrix}0\\V_{bp_3}\\W_{bp_3}\\X_{bp_3}\\Y_{bp_3}\\Z_{bp_3}\end{bmatrix}$$

From the equilibrium of forces acting on the proximal link, i.e., $\mathbf{f}_{dp_i}+\mathbf{f}_{bp_i}=\mathbf{0}\quad(i=1,\ 2,\ 3)$, we have

$$\begin{array}{lll}X_{dp_1}+X_{bp_1}=0 & X_{bp_2}=0 & X_{dp_3}+X_{bp_3}=0\\ Y_{dp_1}+Y_{dp_1}=0 & Y_{dp_2}+Y_{bp_2}=0 & Y_{bp_3}=0\\ Z_{bp_1}=0 & Z_{dp_2}+Z_{bp_2}=0 & Z_{dp_3}+Z_{bp_3}=0\end{array}$$

The balance of moments acting on the proximal link yields, for each leg, three equations and, consequently, for all the legs, nine equations. The vector equilibrium equations, for each leg, with moments about point B_i, are given by

$$\mathbf{m}_{dp_i}+\mathbf{m}_{bp_i}+(\mathbf{n}_{K_i}-\mathbf{n}_{A_i})\times\mathbf{f}_{dp_i}=\mathbf{0},\quad i=1,\ 2,\ 3 \tag{29}$$

We then obtain nine additional scalar equations

$$\begin{array}{lll}U_{dp_1}+U_{bp_1}=0 & U_{bp_2}=0 & U_{bp_3}=0\\ V_{bp_1}=0 & V_{dp_2}+V_{bp_2}=0 & V_{bp_3}=0\\ W_{bp_1}=0 & W_{bp_2}=0 & W_{dp_3}+W_{bp_3}=0\end{array}$$

The wrenches acting at the proximal links are thus

$$\mathbf{w}_{dp_1}=\begin{bmatrix}0\\0\\\sqrt{3}/3)FR_m\\(\sqrt{3}/3)F\\0\\0\end{bmatrix}\qquad \mathbf{w}_{bp_1}=\begin{bmatrix}0\\0\\0\\-(\sqrt{3}/3)F\\0\\0\end{bmatrix} \tag{30}$$

$$\mathbf{w}_{dp_2}=\begin{bmatrix}(\sqrt{3}/3)FR_m\\0\\0\\0\\(\sqrt{3}/3)F\\0\end{bmatrix}\qquad \mathbf{w}_{bp_2}=\begin{bmatrix}0\\0\\0\\0\\-(\sqrt{3}/3)F\\0\end{bmatrix} \tag{31}$$

$$\mathbf{w}_{dp_3}=\begin{bmatrix}0\\(\sqrt{3}/3)FR_m\\0\\0\\0\\(\sqrt{3}/3)F\end{bmatrix}\qquad \mathbf{w}_{bp_3}=\begin{bmatrix}0\\0\\0\\0\\0\\-(\sqrt{3}/3)F\end{bmatrix} \tag{32}$$

Since we assumed that the wrenches are applied at the center of the revolute and cylindrical joints, we determine their effect at the center of the surface of each link end by taking into account the original geometry of the link. Forces are unchanged and moments are given by the relation

$$\mathbf{m}_B=\mathbf{m}_A+(\mathbf{n}_B-\mathbf{n}_A)\times\mathbf{f}_A \tag{33}$$

A safety factor of 1.5, corresponding to a service factor for supporting light machinery, shaft- or motor-driven, according to the

AISC code (Shigley 1989), was taken into account. Furthermore, the loads below, expressed in frame U, were introduced at the surfaces of the proximal links,

$$\mathbf{w}_{dp_1} = \begin{bmatrix} 0 \\ 0 \\ 3.3125 \\ 43.3013 \\ 0 \\ 0 \end{bmatrix} \qquad \mathbf{w}_{bd_1} = \begin{bmatrix} 0 \\ 0 \\ -0.2165 \\ -43.3013 \\ 0 \\ 0 \end{bmatrix} \tag{34}$$

where forces are in N and moments in Nm.

LINK-SHAPE OPTIMIZATION

A two-level approach in the optimization of the proximal links is outlined in the section below: *a*) optimization of the midcurve and *b*) optimization of the link shape.

Optimization of the Midcurve

The optimization of the midcurve of the Agile Wrist was reported earlier (Angeles et al, 2000). For completeness, we include in this subsection an outline thereof.

The midcurve of the proximal link, connecting two points lying at different distances a and b from the center of the sphere, O, is shown in Fig. 4. The shape of the midcurve is to be obtained by means of the concept of *curve synthesis* proposed in (Angeles, 1983) using cubic splines. Because curvature discontinuities induce stress concentrations (Neuber, 1961), we impose the condition that the midcurve be of the G^2-class, i.e., with continuous tangent and continuous curvature everywhere. Additionally, the proximal link is to end on straight segments in order to accommodate the bearings, and hence, the midcurve should blend smoothly with such segments (Fig. 4). The spline-synthesized curve thus should lead to an optimum shape of the link ensuring minimum stress concentrations in the designed link. The geometric requirements imposed on the midcurve Γ are (*i*) to ensure a blending as smooth as possible of the end straight segments with the curved segment; and (*ii*) to minimize the curvature changes throughout Γ.

We can now define the *supporting points* of the midcurve Γ as the set $\{P_k\}_1^N$, with polar coordinates $\{\rho_k, \theta_k\}_1^N$. We thus have to specify angles α and β so that they will yield straight segments of equal length l_0 at the ends of the midcurve. We now have, for $k = 1, \ldots, N-1$,

$$\theta_1 = \alpha, \quad \theta_N = \frac{\pi}{2} - \beta; \tag{35}$$

$$\theta_k = \alpha + \frac{k-1}{N-1}[\frac{\pi}{2} - (\alpha+\beta)]. \tag{36}$$

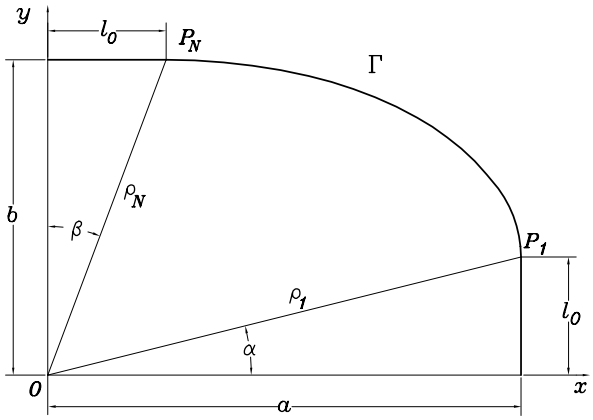

Figure 4. THE MIDCURVE OF THE PROXIMAL LINK

Moreover, we specify

$$\rho_1 = \sqrt{l_0^2 + a^2}, \quad \rho_N = \sqrt{l_0^2 + b^2}. \tag{37}$$

For a fixed value of N, then, we look for $N-2$ values ρ_k, for $k = 2, \ldots, N-1$, that will produce a smooth curve that obeys the conditions for G^2-continuity, namely,

1. its tangent at P_1 should make an angle of $90^\circ - \alpha$ with line OP_1;
2. its tangent at P_N should make an angle of $90^\circ + \beta$ with line OP_N;
3. its curvature should vanish at both P_1 and P_N; and
4. its curvature should have a smooth distribution everywhere.

We recall now the expressions for the angle γ that the tangent of a curve at a point makes with the radius vector at that point (Jeffrey, 1969), and for the curvature κ at a given point, in polar coordinates:

$$\tan\gamma = \frac{\rho(\theta)}{\rho'(\theta)}, \quad \kappa = \frac{\rho^2 + 2(\rho')^2 - \rho\rho''}{(\rho^2 + (\rho')^2)^{3/2}}, \tag{38}$$

where we have used the notation

$$\rho' \equiv \rho'(\theta), \quad \rho'' \equiv \rho''(\theta). \tag{39}$$

Hence, conditions 1 and 2 above take the forms

$$\frac{\rho_1}{\rho_1'} = \tan\left(\frac{\pi}{2} - \alpha\right), \tag{40a}$$

$$\frac{\rho_N}{\rho_N'} = \tan\left(\frac{\pi}{2} + \beta\right). \tag{40b}$$

Additionally, we prescribe zero curvature at points P_1 and P_N:

$$\rho_1^2 + 2(\rho_1')^2 - \rho_1\rho_1'' = 0, \tag{41a}$$
$$\rho_N^2 + 2(\rho_N')^2 - \rho_N\rho_N'' = 0. \tag{41b}$$

In any event, a gradient numerical method will be needed, and hence, derivatives of slope and curvature with respect to the unknowns are required. We therefore use nonparametric splines $\rho = \rho(\theta)$, which lead to partial derivatives with respect to the unknowns that are constant matrices.

Furthermore, we enforce the condition of minimum curvature changes by imposing the minimization of an objective function z that measures the magnitude of the curvature values at the supporting points. Moreover, in order to avoid large curvature changes, we impose an additional constraint: that the curve be *convex*. We can now formulate the optimization problem below:

$$z \equiv \sum_{2}^{N-1} \kappa_k^2 \quad \rightarrow \quad \min_{\mathbf{x}} \tag{42}$$

where $\mathbf{x} \equiv [\rho_2 \quad \cdots \quad \rho_{N-1}]^T$ is the vector of *design variables*, and $\kappa_k \equiv \kappa(\rho_k, \theta_k)$. Moreover, the convexity condition is expressed as

$$\rho_i\rho_{i+1} - 2\rho_{i-1}\rho_{i+1}\cos\Delta\theta + \rho_{i-1}\rho_i \geq 0, \quad i = 2, \cdots, N-1. \tag{43}$$

Note that the conditions 1 and 2 mentioned above were used to impose end conditions for the cubic spline when conditions 3 and 4 were included in the optimization problem as constraints.

When solving the problem, the following values of link parameters were taken from the current design (in mm): $a = 89.5$, $b = 75.5$ and $l_0 = 12.0$.

The solution of the problem described above for $N = 20$ supporting points is displayed in Table 1.

Table 1. NUMERICAL RESULTS FOR THE OPTIMUM MIDCURVE OF THE PROXIMAL LINK

Point No.	ρ	κ
1	90.300900	0.0000000000
2	91.215865	0.0175751286
3	91.984276	0.0183735900
4	92.464602	0.0188806884
5	92.633872	0.0190488823
6	92.484503	0.0188512423
7	92.025255	0.0182888496
8	91.281149	0.0174028281
9	90.291877	0.0162739850
10	89.108383	0.0150138049
11	87.787779	0.0137477721
12	86.387328	0.0125945774
13	84.958746	0.0116465439
14	83.544055	0.0109561503
15	82.173702	0.0105311943
16	80.866940	0.0103386200
17	79.633852	0.0103156475
18	78.478214	0.0103864327
19	77.400404	0.0104809936
20	76.447700	0.0000000000

Optimization of the Cross Section

The optimization of the link cross section along the midcurve obtained above comprises two steps: first, for each given geometry, find the optimum solutions rendering minimum the weight of the link; second, among the solutions, find the one that renders minimum the volumetric strain energy variation. The design variables are the scaling factors defining the size of the cross section of a given shape at points along the midcurve. A link is then created as a solid with size-variable cross section. A discrete set of points is defined along the midcurve, the cross sections at two neighbouring points being obtained by sweeping and blending simultaneously a cross-section to one another to obtain an envelope shape as smooth as possible by using the Pro/Engineer Standard module.

We resort to the FEA by means of the optimization tool in the Structure module of Pro/Mechanica, using aluminium AL2014. The objective function is given as the weight of the link subject to limits on the maximum and minimum principal stresses, the von Mises stress, and the shear stress components. Due to the complexity of the model and the high number of variables involved, the optimization module could not even finish the first iteration. We then handled the problem recursively, by increasing the number of size-variable cross sections from two until the mass difference between two successive iterations became negligible: for a given cross-section shape, the aim was then to determine the minimum number of variable sections required to obtain the optimum shape. Between the two successive shapes obtained before, we keep the one that minimizes the strain energy variation and keep

also the shape satisfying the same criterion among all the optimum shapes.

Figure 5 depicts the location of the first five variable sections and Fig. 6 shows the different cross-section shapes tested. It was found that, for any of the shapes of Fig. 6, the mass difference was insignificant when the number of variables exceeded five. Moreover, with some cross sections, such as the "I-beam" and the "round-square", we were not able to find a solution. In others, such as the elliptical section, the results led to too heavy links. Optimum circular cross sections were not easy to find either.

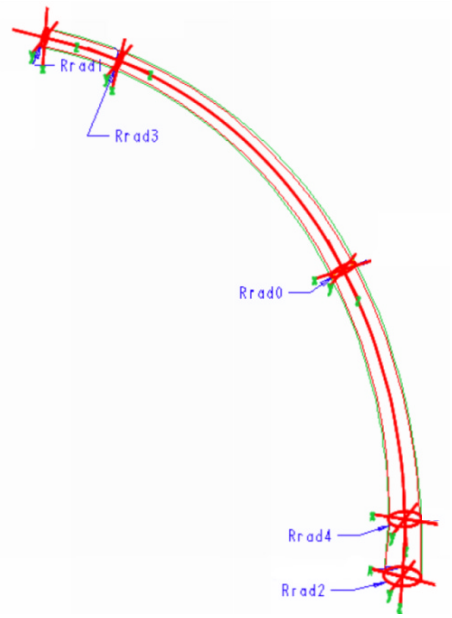

Figure 5. PROXIMAL LINK WITH VARIABLE CIRCULAR CROSS-SECTIONS

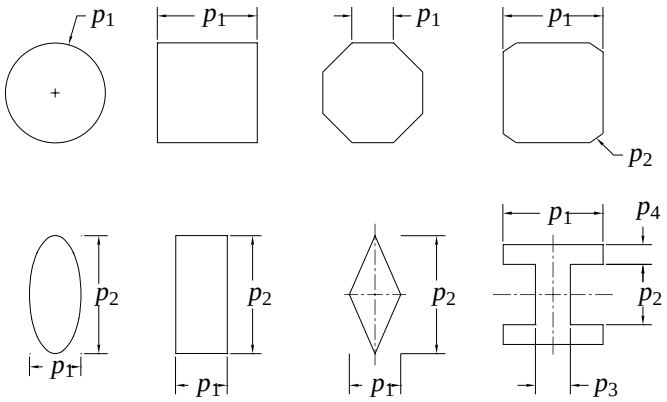

Figure 6. THE VARIOUS CROSS SECTIONS TESTED

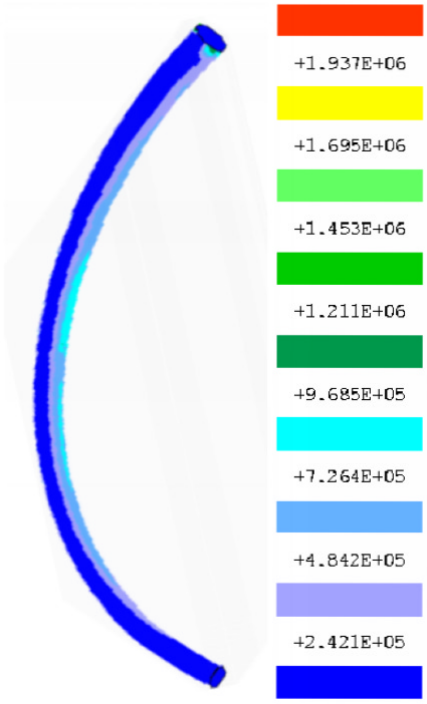

Figure 7. STRAIN ENERGY INSIDE THE OPTIMUM SHAPE WITH TWO CIRCULAR CROSS SECTIONS

It is worth mentioning that we narrowed the geometrical boundaries of the design variables in order to speed up the convergence. Among the different types of sections tested, the circular and rectangular shapes reported better solutions in terms of weight. However, while comparing the stress and the strain energy in the proximal links for the two different sections, the circular cross-section turns out to have a more homogeneous stress distribution, with a strain energy per unit volume close to constant. Comparisons are shown in Figs. 7 & 8. Moreover, this result matches the Venkayya criterion (Venkayya, 1971), according to which the optimum design is the one in which the strain energy per unit volume is constant. Another interesting observation is that the stress along the midcurve is at its lowest level at every cross section.

As we can see in Figs. 9 & 10, the optimum shapes found when increasing the number of parameters (that is, the number of sections) from two to five for the circular link are geometrically very close. The proximal link with only two variable sections has a better homogeneity regarding stress and strain energy since the simultaneous blending and sweeping from the first section to the second is smoothest. For this reason we decided to use the shape with two circular sections as an initial shape for the proximal link.

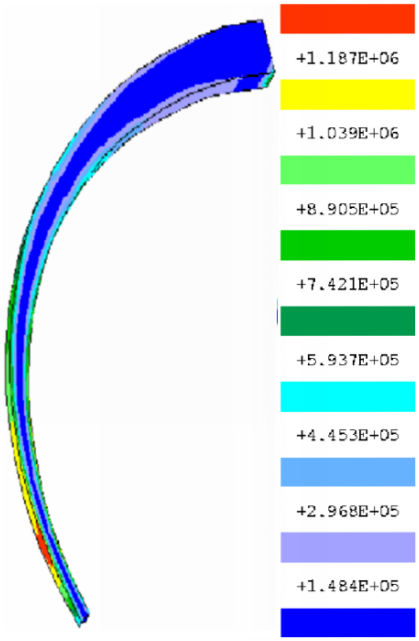

Figure 8. STRAIN ENERGY INSIDE THE OPTIMUM SHAPE WITH TWO RECTANGULAR CROSS SECTIONS

Table 2. RESULTS USING CIRCULAR CROSS-SECTION WITH TWO AND FIVE DESIGN VARIABLES

# of sections	2	5
r_1 (mm)	1.526	1.487
r_2 (mm)	2.619	1.543
r_3 (mm)		2.134
r_4 (mm)		2.505
r_5 (mm)		2.861
Weight(g)	4.591	4.411

Results of the optimization for this shape are listed in Table 2. To design the straight end, whose form was fixed as a rectangular parallelepiped, we inscribed the circular section in a square whose edge length is slightly bigger than the biggest diameter obtained for the two links, in order to allow for a fillet to avoid stress concentrations.

In addition, the design of the cross section of the distal links was conducted using the same approach described above. The optimum solutions obtained indicated a very small variation in the size of the cross section along its midcurve, i.e., the cross section is almost uniform. Therefore, in order to reduce the manufacturing cost, we adopted a uniform cross section in the design of the shape of the distal links.

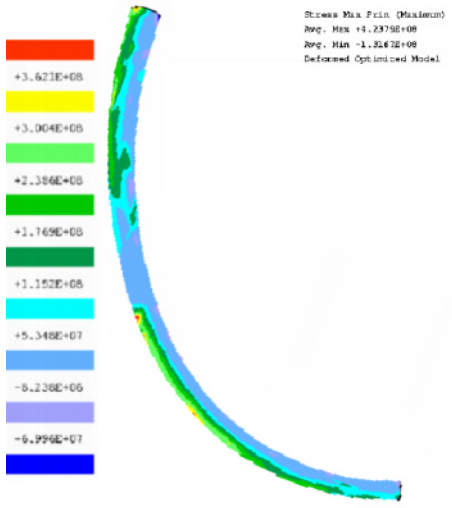

Figure 9. MAXIMUM STRESS IN THE OPTIMUM SHAPES WITH TWO CIRCULAR CROSS SECTIONS

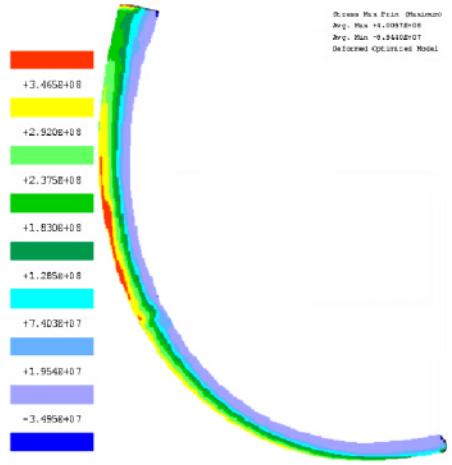

Figure 10. MAXIMUM STRESS IN THE OPTIMUM SHAPES WITH FIVE CIRCULAR CROSS SECTIONS

CONCLUSIONS

We introduced a two-level approach to the optimum design of the proximal links of a parallel spherical manipulator, the *Agile Wrist*. In this approach, we first determined the link midcurve by means of cubic splines, while minimizing the curvature variations so that the stress concentration was minimized. In the sec-

Table 3. THE OPTIMUM SOLUTIONS.

max principal stress	4.2369×10^8 Pa
max von Mises stress	3.9357×10^8 Pa
max *xx* stress	3.9043×10^8 Pa
max *xy* stress	7.3325×10^7 Pa
max *xz* stress	1.9263×10^8 Pa
max *yy* stress	1.5218×10^8 Pa
max *yz* stress	1.5718×10^8 Pa
max *zz* stress	2.9715×10^8 Pa
min principal stress	3.6762×10^8 Pa
# of shells	8
# solids	171
Total Elapsed Time	741.08 s
Total CPU Time	275.01 s
Max Memory Usage	86976 kilobytes

ond level, we found the size of the cross-section along the mid-curve. We resorted to a finite element analysis using ProMechanica, the optimum geometries being obtained by trying different cross-sections. The results obtained showed a substantially uniform distribution of strain energy per unit volume along the proximal link, which verifies Venkayya's criterion.

ACKNOWLEDGEMENTS

The parallel wrist was developed thanks to a NSERC (Canada's Natural Sciences and Engineering Research Council) equipment grant obtained in the 1998 competition; this work is also partly supported by NSERC under Strategic Project 215729-98. The first author conducted her share of the work reported here while on a visit at McGill's Centre for Intelligent Machines, on leave from France's Ecole Centrale de Nantes' Institut de Recherches en Cybernétique et Communications de Nantes.

REFERENCES

Angeles, J., "Synthesis of plane curves with prescribed geometric properties using periodic splines", *Computer-Aided Design*, vol. 15, No. 3, pp. 147–155, 1983.

Angeles, J., Jabre, L., Slutski, L., St-Jean, M., and Teng, C. -P., "The design of a three-DOF parallel robotic wrist", *IDMME 2000 Conference*, May, 2000.

Angeles, J., Morozov, A., Slutski, L., Pizarro, A., Navarro, O., and Jabre, L., "A modular approach to the mechanical design of a macro-micro manipulator system for the servicing and maintenance of aircraft (M^3 system)," *Technical Report TR-CIM-99-12*, Centre for Intelligent Machines, McGill University, Montreal, Canada, 1999.

Brand, L., *Advanced Calculus*, New York, John Wiley & Sons, Inc., 1965.

Gosselin, C.M. and Lavoie, E., "On the kinematic design of spherical three-degree-of-freedom parallel manipulators," *The Int. J. of Robotics Research*, vol. 12, No. 4, pp. 394–402, 1993.

Gosselin, C.M. and Hamel, J.-F., "The agile eye: A high-performance three-degree-of-freedom camera-orienting device," *Proc. IEEE Int. Conf. Robotics and Automation*, San Diego, pp. 781–786, 1994.

Gosselin, C.M. and Gagné, M., "A closed-form solution for the direct kinematics of a special class of spherical three-degree-of-freedom parallel manipulators," in J.-P. Merlet and B. Ravani, eds. *Computational Kinematics*, Proc. of the Second Workshop on Computational Kinematics," Kluwer Academic Publishers, Dordrecht, pp. 231–240, 1995.

Jeffrey, A., *Mathematics for Engineers and Scientists*, London, Nelson, 1969.

Larochelle, P. and McCarthy, J. M., "Static analysis of spherical nR kinematic chains with joint friction", *ASME Flexible Mechanisms, Dynamics and Analysis*, Vol. 47, pp. 173–177, 1992.

Neuber, H., *Theory of Notch Stresses: Principles for Exact Calculation of Strength with Reference to Structural Form and Material*, 2nd ed., Washington, U.S. Dept. of Commerce, Office of Technical Services, 1961.

Shigley, J. E., *Mechanical Engineering Design*, New York, McGraw-Hill, 1989.

Teng, C.-P. and Angeles, J., "A sequential-quadratic-programming algorithm using orthogonal decomposition with Gerschgorin stabilization", *ASME J. Mechanical Design*, to appear, 2000.

Venkayya, V.B., "Design of the optimum structure", *Computers and Structures*, Vol. 1, pp. 263-309. 1971,

Yi, B. -J., Freeman, R. A., and Tesar, D., "Force and stiffness transmission in redundantly actuated mechanisms: the case for a spherical shoulder mechanism", *Proceedings of ASME Robotics, Spatial Mechanisms, and Mechanical Systems Conferences*, DE-Vol. 45, pp. 163-172, 1992.